MORPHOLOGICAL AND COMPOSITIONAL INVESTIGATION OF KRIEGER CRATER (MOON)

C. Collu [1*], S. Podda [1], M.T. Melis [1,]

[1] Dept. of Chemical and Geological Sciences, University of Cagliari, Monserrato, Italy

KEY WORDS: Planetary geology, Moon, Spectroscopy, Krieger crater, Surface

ABSTRACT:

Krieger crater is an impact lunar crater located in the Oceanus Procellarum, on the western near-side of the Moon. It is partly overlaid by Van Biesbroeck impact crater on the southern rim; a sinuous rille, Rima Krieger, originates from the western rim. Krieger is surrounded by wrinkle ridges, linear structural features, and different mare materials. In order to investigate the geomorphological setting, we used remote sensing datasets from Lunar Reconnaissance Orbiter and Kaguya for photogeological and topographic analysis through high-resolution imagery and DEM, and Moon Mineralogy Mapper hyperspectral data for surface compositional investigation. Krieger is characterized by a polygonal-shaped rim, an asymmetrical ejecta blanket, oriented north-south (indicating a potential oblique impact) and a complex floor configuration, with morphologic features, like hummocks, large mounds, a possible central peak, and unclear concentric fractures. Both Krieger and Van Biesbroeck walls exhibit melt coating features, fresh exposed materials, melt veneers, and mass wasting morphologies. Hyperspectral analysis determined several surface mineral compositions, differing especially in olivine and glass content. Important compositional differences were observed in the Krieger floor, where mare-like basalts have been detected, suggesting an internal post-impact volcanism which resulted in the breaching of the western rim and subsequent lava flow outside the crater, originating Rima Krieger. We found also the contamination of highland material in the southern ejecta, potentially derived from the Aristarchus crater impact. Thus, this complex geological setting suggests that post-impact modification processes, including volcanism, tectonic movements and later impacts, played a key role in shaping up the present Krieger crater.

1. INTRODUCTION

Impact craters are the most common surface features on many solid planets, including Earth's Moon. Based on the diameter size, craters can be classified in simple craters (< 15 km) and complex craters (>20 km). Krieger is an Imbrian complex crater, that has a diameter of ~ 25 km. It is located in the Oceanus Procellarum, on the western near-side of the Moon, in the Aristarchus-Harbinger Region (Figure. 1), known as the most geologically complex region of the Moon (Zisk, et al., 1977). In this work, remote sensing data from Lunar Reconnaissance Orbiter (LRO), Kaguya and Chandrayaan-1 missions have been used to investigate the surface morphology and composition of Krieger crater, in order to better understanding the geological processes that affected the present appearance of the crater.

2. DATA AND PROCESSING

Narrow Angle Cameras (NAC) high resolution images from LRO mission, the Digital Elevation Model (SLDEM2015), and Moon Mineralogy Mapper (M3) reflectance data (Chandrayaan-1 mission) were used in this work. All data were downloaded from the Planetary Data System (PDS) Geosciences Node Lunar Orbiter Data Explorer.

High resolution images from NAC are 8-bit panchromatic imagery, with a spatial resolution of ~0.5 m/pixel. In this work we used 40 calibrated NAC images from CDRNAC data products, with sun incidence angles range from 0° to 80°, in order to observe surface reflectance variations and/or recognize morphological features enhanced by shadows.

SLDEM2015 consists of a co-registered data from geodetically-accurate topographic heights of the Lunar Orbiter Laser Altimeter (LOLA) onboard the Lunar Reconnaissance Orbiter

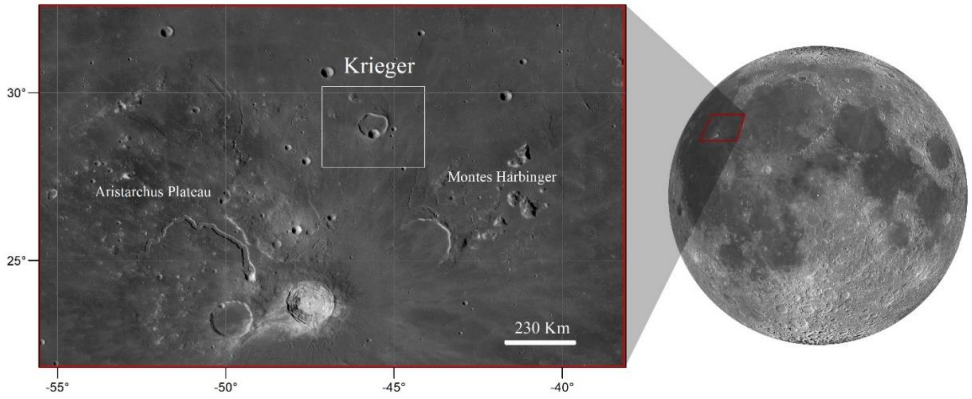

Figure 1. A portion of LRO Wide Angle Camera (WAC) mosaic showing the study area. Krieger crater (enclosed in the white rectangle) is located in the Aristarchus-Harbinger Region, in the Oceanus Procellarum, centered at ~ (29.0°N, 45.6°W).

* Claudia Collu, claudiacollu26@yahoo.it

and, 43,200 stereo-derived DEMs (each) from the SELENE Terrain Camera (TC) (~1010 pixels total) (Barker, et al, 2016). This DEM has a spatial resolution of 512 pixels per degree (~60 m at the equator) and a vertical accuracy of ~3 to 4 m. For this study we used two mosaicked tiles: "SLDEM2015_512_00N_30N_270_315" and "SLDEM2015_512_00N_30N_270_315".

We used global mode photometrically calibrated reflectance data (REFIMG) of Moon Mineralogy Mapper (M3), in particular the "M3G20090209T033051_V01_RFL" imagery. M3 reflectance data covers the wavelength range from 430 nm to 3000 nm with a spatial resolution of ~ 140 m/pixel, and the spectral resolution of 20-40 nm. The reflectance image has been processed in IDL-ENVI software, performing first a spatial and spectral resize, in order to exclude areas of no interest. Moreover, data with wavelength beyond 2600 nm, affected by thermal emission component, that makes difficult the analysis of adsorption features (Clark, 1979), have been ignored. Then, noise reduction was carried out using Maximum Noise Fraction (MNF) method.

3. METHODS

Geomorphological investigation of Krieger crater region has been mainly performed through photogeological observations from NAC high resolution images, that include albedo variations, surface texture analysis and identification of distinctive geologic features; the SLDEM2015 has been used for landscape analysis, through topographic sections and 3D visualizations, especially for define crater rims morphology.

Surface compositional analysis has been carried out on M^3 reflectance data, in order to define spatial distribution of distinct compositional units in the study area. A preliminary investigation was performed by calculating three spectral parameters used in several studies (Pieters, 1978; Staid, et al., 2011), and combining them in an RGB colour composite map: the 1 and 2 μm band depths (assigned in red and green channel respectively) and the reflectance at 1,58 μm (blue channel).

Then, we used RGB composite map as a guide for identify regions of compositional interest and collect characteristic spectra, in order to build a spectral library that describes the Krieger region. Further spectra were collected through ENVI Pixel Purity Index (PPI) algorithm. Thus, in order to identify spatial distribution of the reference spectra of the library, we used ENVI Spectral Angle Mapper (SAM) algorithm, assigning a different maximum angle to each spectrum, with values between 0,02 and 0,1 radians, based on the presence of residual noise, that could affect the classification. In addition, we investigated individually all the library spectra, analysing continuum slopes, band minimum position, band depth, band width and symmetry of spectral adsorptions, related to mineral composition (Singer, 1981; Cloutis, et al., 1986; Horgan, et al., 2014). However, in order to enhance spectral absorption features before this analysis, continuum of the spectra was removed (McCord, et al., 1981; Horgan, et al., 2014). We considered a linear continuum broken in two segments with three tie points at 730, 1209 or 1578 and 2616 nm for pyroxene-dominant compositions, whereas for olivine-rich compositions

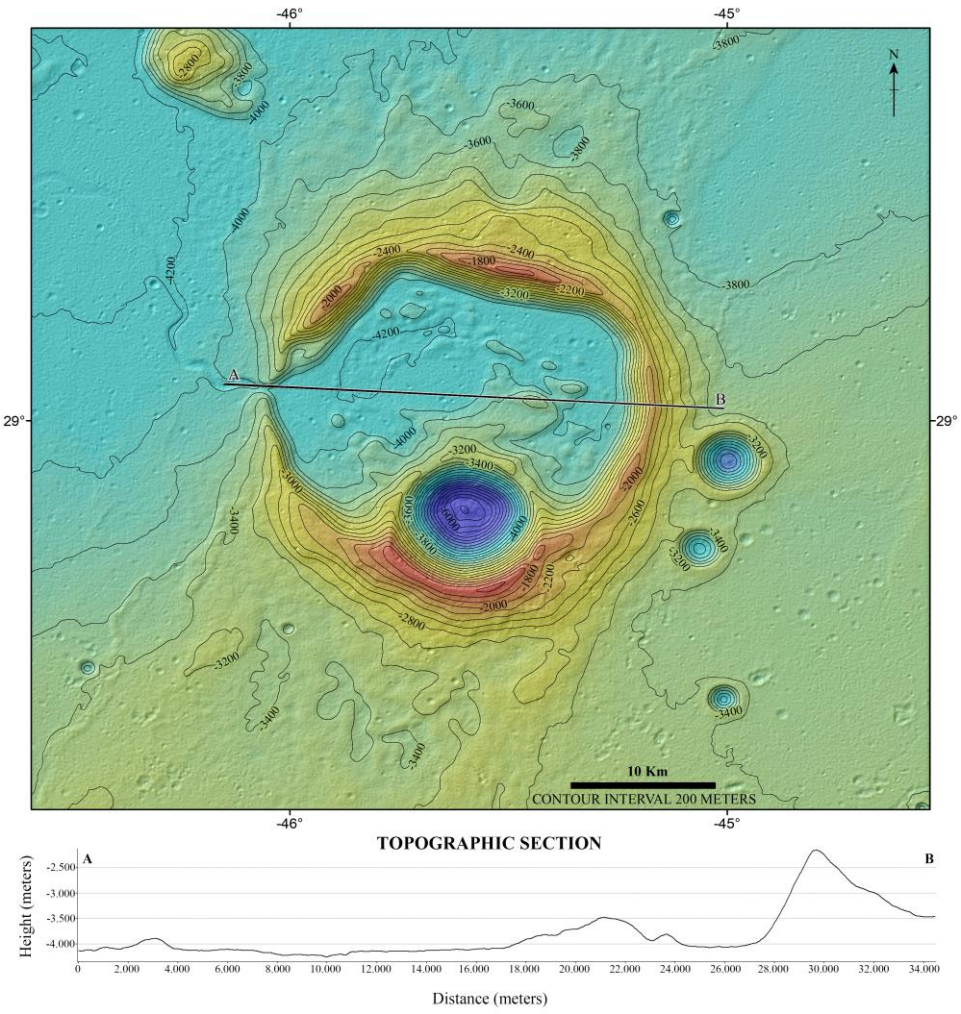

Figure 2. Topographic map and topographic section extracted from SLDEM2015; contour interval: 200 meters.

we adjusted tie points at 700, 1778 and 2616 nm, because olivines exhibit a broad 1 µm band adsorption, centred at longer wavelengths (Sunshine & Pieters, 1998; Horgan, et al., 2014). Continuum removal was achieved by dividing the continuum into the actual spectrum.

4. RESULTS

The Krieger crater shows a polygonal-shaped rim, with the southern part partly overlaid by a smaller Eratosthenian simple crater, Van Biesbroeck, and an asymmetric ejecta blanket, characterized by a north-south orientation. A rille, Rima Krieger, extends from the breached western rim out of the crater, at first with deep and angular meanders, suggesting the presence of different substratum material and/or a control by underlying structures (Podda, et al., 2020). To the southeast of Krieger two small Eratosthenian craters are located, Rocco and Ruth. Furthermore, Krieger is surrounded by several wrinkle ridges trending north-northeast to south-southwest.

NAC images show in the crater a significant albedo variation between northern and southern areas, probably related to different surface compositions. Moreover, further observations through NAC imagines revealed a complex floor configuration, with the presence of unclear concentric linear features, hummocks, large mounds (isolated or in clusters) and a possible central peak, characterized by a rougher surface texture and a higher crater density compared with the other reliefs. Crater walls of both Krieger and Van Biesbroeck exhibit melt coating features and frequent scarps in the upper part, whereas several mass wasting morphologies like boulder rolling features and block deposits occur in the lower areas. Between these wall units, a more coherent material is exposed, covered by dark thin melt veneers and coarse depositional materials “debris flows”, often with boulder-rich termination deposits.

Topography analysis through SLDEM2015 shows that in the Krieger crater region heights range between -6321 and -1328 meters, with general slope trending towards north-west. Morphology of Krieger was investigated through topographic sections, revealing an average rim-to-rim diameter of ~ 25,2 km, average depth of ~ 557,7 meters (below the pre-existing surface) and average rim height of ~ 1409,6 meters (above pre-existing surface); western breached wall shows a rim height almost 2 km lower (Figure 2). A marked asymmetry in rim height was found also between Van Biesbroeck’s northern and southern rim, that is almost 1,7 km higher; this asymmetry can be due to the irregular pre-impact topography, represented by the rim of Krieger. Moreover, in the north-western wall of Krieger a sudden slope decrease has been detected, and interpreted as a distinctive landslide deposit. On Krieger floor the large mounds and reliefs range from 1 to 4 km in diameter, heights between 30 m and 400 m, with slopes ranging from 20° to 40°. Outside the Krieger crater, ejecta blanket morphology is asymmetrical, with the northern deposits clearly thicker than southern ones. This difference could be related to variations in the pre-existing topography or post-impact modification triggered by nearby wrinkle ridges.

Preliminary spectral analysis through RGB colour composite map (Figure 3b) allowed the identification of fundamental characteristics of surface composition. The yellow hues in the southern areas and northern Krieger ejecta show both 1 and 2 µm strong adsorptions, indicating a pyroxene-dominant composition (Cloutis, et al., 1991; Staid, et al., 2011; Horgan, et al., 2014). On the contrary, blue/cyan hues in the southern ejecta of Krieger are characterized by high albedo and weak 1 µm adsorption, suggesting a less mafic compositions, typical of highlands. Red hues located in northern areas suggest strong adsorption band near 1 µm and relatively weak 2 µm absorption, typical of olivine-dominant compositions (Staid, et al., 2011; Sunshine & Pieters, 1998). In addition, 17 characteristic spectra of the Krieger crater region were collected and investigated (Figure 3d). All spectra show the typical reddening, due to fine Fe^0 particle sizes and space weathering (Pieters, 1978; Horgan, et al., 2014). Spectral signatures from B1 to VE2 (from top to bottom in figure 3d) clearly represent soils (regolith), since they have much weaker adsorption features than the other signatures, that characterize fresh rock materials on crater walls. Moreover, most of the signatures present the 1 µm band minimum at 0,98 or 1,09 and the 2 µm

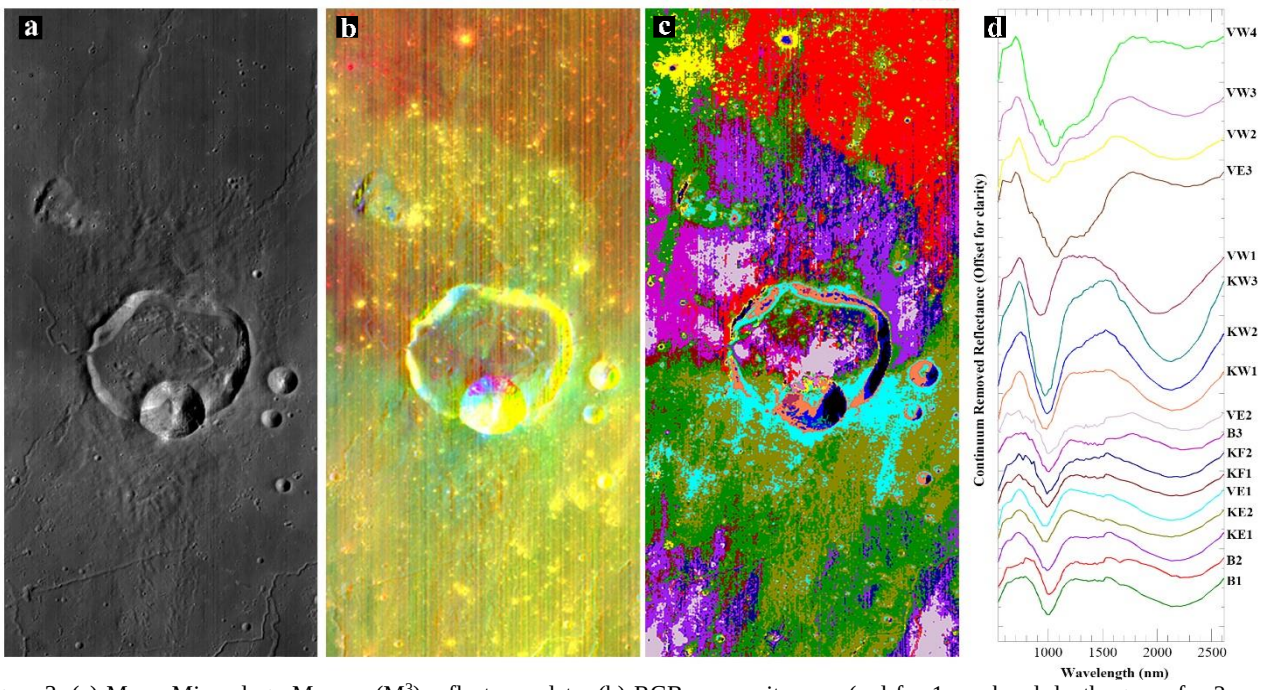

Figure 3. (a) Moon Mineralogy Mapper (M^3) reflectance data; (b) RGB composite map (red for 1 µm band depth, green for 2 µm band depth, blue for reflectance at 1.58 mm); SAM classification (c) and relative continuum removed spectral signatures (d) of the Krieger crater region.

band minimum at 2,14 or 2,22 µm, consistent with a Clinopyroxene (CPX)-rich composition, likely mixed with Orthopyroxene (OPX). However, the position of band minimum at longer wavelengths could also be due to a higher content in glass (Tomkins & Pieters, 2010). On the contrary, VW1 has band adsorptions centred at 0,93 and 2,02 µm, suggesting an OPX-dominant composition. The analysis of 1 µm band configuration (width and symmetry) allows to discriminate olivine rich-compositions. VW4 has an almost pure olivine signature, characterized by a broad and asymmetric band adsorption centred near 1,06 µm, and a very weak 2 µm band. VW2, VW3, and VE2 have stronger 2 µm band adsorption and broad asymmetric 1 µm band adsorption, both centred at longer wavelength compered to pyroxene-dominant compositions, suggesting an olivine-pyroxene mixture mineralogy, with possible glass content. Olivine presence was identified also in crater walls covered by melt veneers (KW2 and KW3), even though in less abundance compared to VW2, VW3, and VE2, and in soils (B2, KE1, KF2, B3 and VE2), that show the highest values of 1µm band asymmetry of soil signatures. On the contrary, soils lacking of olivine are represented by B1, KF1, KE2 and VE1 signatures, that show pyroxene-dominant composition, with possible contamination by highland components, including feldspar and Mg-Spinels, particularly for KE2 and VE1 (Cheek & Pieters, 2014).

5. CONCLUSIONS

Geomorphologic and spectral analysis of Krieger crater revealed several landforms and surface mineralogic compositions. The shape of rims and ejecta blanket suggest that Krieger likely formed as a result of an oblique impact on a mare basalt poor in olivine. The complex floor configuration and the presence of mare-like materials rich in olivine (B3) suggest intense post-impact modification processes, typical of floor fractured craters (Schultz, 1976), including floor uplift and volcanism triggered by the intrusion of a magma chamber beneath the crater. These processes are probably responsible of the development of concentric fractures, hummocks and mounds. Volcanic eruptions partly inundated the Krieger floor, leading to the breach of western rim and subsequent emplacement of basalts outside the crater. Then, the impact that generated Van Biesbroeck excavated Krieger floor and exposed deep materials rich in olivine, detected in the northern walls and ejecta of Van Biesbroeck. Later, southern materials of the Krieger region have been contaminated with highland components derived from Aristarchus ejecta. Thus, post-impact modification processes, including tectonic movements, volcanism and later impacts, played a key role in shaping up the present Krieger crater.

REFERENCES

Barker M.K., Mazarico E., Neumann G.A., Zuber M.T., Haruyama J., Smith D.E. (2016). A new lunar digital elevation model from the Lunar Orbiter Laser Altimeter and SELENE Terrain Camera. *Icarus*, vol. 273,2016. Pages 346-355. ISSN 0019-1035. Doi:10.1016/j.icarus.2015.07.039

Cheek, L. C., & Pieters, C. M. (2014). Reflectance spectroscopy of plagioclase-dominated mineral mixtures: Implications for characterizing lunar anorthosites remotely. *American Mineralogist*, vol. 99, doi:10.2138/am-2014-4785

Clark, R. N. (1979). Planetary reflectance measurements in the region of planetary thermal emission. *Icarus*, vol. 40, no. 1, Art. no. 1, doi:10.1016/0019-1035(79)90056-3

Cloutis, E. A., & Gaffey, M. J. (1991). Pyroxene spectroscopy revisited: Spectral-compositional correlations and relationship to geothermometry. *Journal of Geophysical Research*, vol. 96, no. E5, Art. no. E5. doi:10.1029/91je02512

Cloutis, E. A., Gaffey, M. J., Jackowski, T. L., & Reed, K. L. (1986). Calibrations of phase abundance, composition, and particle size distribution for olivine-orthopyroxene mixtures from reflectance spectra. *Journal of Geophysical Research*, vol. 91, no. B11, Art. no. B11. doi:10.1029/jb091ib11p11641

Horgan, B. H., Cloutis, E. A., Mann, P., & Bell, J. F. (2014). Near-infrared spectra of ferrous mineral mixtures and methods for their identification in planetary surface spectra. *Icarus*, vol. 234, 132–154. doi:10.1016/j.icarus.2014.02.031

McCord, T. B., Clark, R. N., Hawke, B. R., McFadden, L. A., Owensby, P. D., Pieters, C. M., & Adams, J. B. (1981). Moon: Near-infrared spectral reflectance, A first good look. *Journal of Geophysical Research: Solid Earth*, vol. 86, no. B11, Art. no. B11. doi:10.1029/jb086ib11p10883

Pieters, C. M. (1978). Mare basalt types on the front side of the Moon: a summary of spectral reflectance data. *Proc. Lunar Planet. Sci. Conf. 9th*, 2825–2849.

Podda, S., Melis, M. T., Collu, C., Demurtas, V., Perseu, F. O., Brunetti, M. T., & Scaioni, M. (2020). New Morphometric Data of Lunar Sinuous Rilles. *IEEE Journal of Selected Topics in Applied Earth Observations and Remote Sensing*, vol. 13, 3304–3316. doi:10.1109/jstars.2020.3003080

Schultz, P. H. (1976). Floor-fractured lunar craters. *The moon*, vol. 15, no. 3, Art. no. 3. doi:10.1007/BF00562240

Singer, R. B. (1981). Near-infrared spectral reflectance of mineral mixtures: Systematic combinations of pyroxenes, olivine, and iron oxides. *Journal of Geophysical Research: Solid Earth*, doi:10.1029/jb086ib09p07967

Staid, M. I., Pieters, C. M., Besse, S., Boardman, J., Dhingra, D., Green, R., Taylor, L. A. (2011). The mineralogy of late stage lunar volcanism as observed by the Moon Mineralogy Mapper on Chandrayaan-1. *Journal of Geophysical Research: Planets*, doi:10.1029/2010JE003735.

Sunshine, J. M., & Pieters, C. M. (1998). Determining the composition of olivine from reflectance spectroscopy. *Journal of Geophysical Research: Planets*, doi:10.1029/98je01217

Tomkins, S., & Pieters, C. M. (2010). Spectral characteristics of lunar impact melts and inferred mineralogy. *Meteoritics & Planetary Science*, doi:10.1111/j.1945-5100.2010.01074.x

Zisk, S. H., Hodges, C. A., Moore, H. J., Shorthill, R. W., Thompson, T. W., Whitaker, E. A., & Wilhelms, D. E. (1977). The Aristarchus-Harbinger region of the moon: Surface geology and history from recent remote-sensing observations. *The moon*, vol. 17, no. 1, Art. no. 1. doi:10.1007/BF00566853